

September 1996

# BARYON DENSITY AND THE DILATED CHIRAL QUARK MODEL

Youngman Kim and Hyun Kyu Lee

*Department of Physics, Hanyang University  
Seoul, Korea*

## Abstract

We calculate perturbatively the effect of density on hadronic properties using the chiral quark model implemented by the QCD trace anomaly. We calculate the density dependent masses of the constituent quark ( $m_Q$ ), the scalar field ( $m_\chi$ ) and the pion ( $m_\pi$ ) in one-loop order using the technique of thermo field dynamics. In the chiral limit, the pion remains massless at finite density. It is found that the tadpole type corrections lead to the decreasing masses with increasing baryon density, while the radiative corrections induce Lorentz-symmetry-breaking terms except when the particles probed is of high energy. We found in the large  $N_c$  limit (large scalar mass limit) that

tadpoles dominate and the mean-field approximation is reliable, giving rise a Lorentz-invariant Lagrangian with masses decreasing as the baryon density increases.

# 1 *Introduction*

One of the most challenging current topics in hadronic physics is to understand how physical properties of nuclear matter change as density (or temperature) is increased toward the chiral phase transition predicted to take place at some critical density  $\rho_c$  (or critical temperature  $T_c$ ). We know quite a lot from chiral perturbation theory and lattice QCD calculations what happens as temperature is raised in the absence of baryon density but very little is known from first principles what happens as density is increased. Understanding how density affects nuclear dynamics is essential for several important issues of physical phenomena: Neutron stars involve dense matter at low temperature while relativistic heavy-ion collisions probe primarily hot matter in dense medium. Even in ultrarelativistic heavy-ion collisions such as at RHIC, density is expected to play a major role, so it needs to be incorporated in the calculations to confront experiments. At present, the only tool available to study density effects is the effective Lagrangian approach.

It has been suggested by Brown and Rho [1] that the scale anomaly of QCD suitably incorporated into an effective chiral Lagrangian allows one to study dense-medium effects in a simple mean-field approximation provided the parameters of the Lagrangian scale in medium. The predicted scaling law (called “BR scaling”) has been found to be consistent with a variety of nuclear phenomena [2, 3, 4]. As discussed in [2], there is a close relation between the physics of BR scaling and that of the dilated chiral quark model (DCQM) of Beane and van Kolck [5]. Starting from a nonlinear  $\sigma$  model of constituent quarks and pions that incorporates the QCD scale anomaly, Beane and van Kolck[5] showed that the “mended symmetry” of Weinberg [6] can be realized in the dilaton limit with the effective Lagrangian becoming a linearized  $\sigma$ -model. Thus the Beane-van Kolck model in the dilaton limit is to describe in some qualitative and heuristic way the state of matter near the chiral phase transition much as BR scaling is to describe the “dropping” hadron masses near the phase transition [7]. In [8], this aspect of the DCQM was exploited to predict the temperature dependence of hadronic properties near the phase transition: this calculation confirms what has always been tacitly assumed, namely, a more rapid decreasing of  $f_\pi$ ,  $m_\sigma$ , and  $m_Q$  with temperature in the presence of matter density compared with the zero-density  $\sigma$  model. This prediction – which is hardly a surprise – is actually consistent with what is observed in heavy-ion experiments [9].

In all above developments, the question as to how relevant the dilaton limit is to dense nuclear matter was not, however, properly addressed. It was simply assumed in [8] that the Lorentz-invariant dilated chiral quark model (DCQM) embodying Weinberg’s mended symmetry describes correctly the state of matter near the chiral phase transition where the  $O(4)$  chiral symmetry is presumably restored. The question then is: how useful is this Lagrangian away from the phase transition point (e.g., nuclear matter) and how can one arrive at this form of Lagrangian starting from a zero-density effective Lagrangian of QCD ? In this paper, we make a first attempt to answer this question. For this purpose, we calculate perturbatively the effect of density on hadronic properties using the original Lagrangian from which Bean and van Kolck derive in the dilaton limit the dilated chiral quark model. Specifically we calculate the density-dependent masses of the constituent quark ( $m_Q$ ), the scalar field ( $m_\chi$ )<sup>1</sup> and the pion ( $m_\pi$ ) in one-loop order using the technique of thermo field dynamics. The basics of the thermo field dynamics are summarized in Appendix I. Since we are interested mostly in density effects, we take the low-temperature limit and focus on the parts that explicitly depend on the density. We discuss the physical relevance of the Lorentz-invariant dilated chiral quark Lagrangian when applied to dense matter. Of course, Lorentz invariance is clearly broken in the presence of matter density. So the question is to what degree the dilated chiral quark model could be a good approximation to dense nuclear matter [2].

## 2 *Effective Lagrangian*

The effective chiral-quark Lagrangian implemented with the QCD conformal anomaly is

$$\begin{aligned}
L &= \bar{\psi}i(\not{\partial} + \not{V})\psi + g_A\bar{\psi} \not{A}\gamma_5\psi - \sqrt{\kappa}\frac{m}{f_\pi}\bar{\psi}\psi\chi + \frac{1}{4}\kappa tr(\partial_\mu U\partial^\mu U^\dagger)\chi^2 \\
&+ \frac{1}{2}\partial_\mu\chi\partial^\mu\chi - V(\chi) + \dots
\end{aligned} \tag{1}$$

where  $\kappa \equiv \frac{f_\pi^2}{f_d^2}$ ,  $V_\mu = \frac{1}{2}(\xi^\dagger\partial_\mu\xi + \xi\partial_\mu\xi^\dagger)$ ,  $g_A = 0.752$  is the axial-vector coupling

---

<sup>1</sup>The scalar field that figures in the dilaton limit must be the quarkonium component that enters in the trace anomaly, not the gluonium component that remains “stiff” against the chiral phase transition. See [2] for a discussion on this point.

constant for the constituent quark and  $A_\mu = \frac{1}{2}i(\xi^\dagger \partial_\mu \xi - \xi \partial_\mu \xi^\dagger)$  with  $\xi^2 = U = \exp(\frac{i2\pi_i T_i}{f_\pi})$ . The potential term

$$V(\chi) = -\frac{\kappa m_\chi^2}{8f_\pi^2} \left[ \frac{1}{2} \chi^4 - \chi^4 \ln\left(\frac{\kappa \chi^2}{f_\pi^2}\right) \right]. \quad (2)$$

reproduces the trace anomaly of QCD at the effective Lagrangian level.<sup>2</sup> We assume that this potential chooses the ‘‘vacuum’’ of the broken chiral and scale symmetries.

After spontaneous chiral symmetry breaking (i.e.,  $\chi \rightarrow f_d + \chi$ ), eq.(1) becomes

$$\begin{aligned} L = & \bar{\psi} i(\not{\partial} + \not{V})\psi + g_A \bar{\psi} A \gamma_5 \psi - m \bar{\psi} \psi - \frac{m}{f_d} \bar{\psi} \psi \chi \\ & + \frac{1}{4} \frac{f_\pi^2}{f_d^2} \text{tr}(\partial_\mu U \partial^\mu U^\dagger) (f_d + \chi)^2 + \frac{1}{2} \partial_\mu \chi \partial^\mu \chi - V(f_d + \chi) + \dots \end{aligned} \quad (3)$$

Expanding  $U$  in terms of pion fields and collecting the terms relevant for one-loop corrections, the Lagrangian can be written

$$\begin{aligned} L = & \bar{\psi} i \not{\partial} \psi - m \bar{\psi} \psi - \frac{m}{f_d} \bar{\psi} \psi \chi \\ & + \frac{1}{2} \partial_\mu \pi \partial^\mu \pi - \frac{g_A}{f_\pi} \bar{\psi} \not{\partial} \pi \gamma_5 \psi - \frac{1}{2f_\pi^2} \epsilon_{abc} T_c \bar{\psi} \not{\partial} \pi^a \pi^b \psi \\ & + \frac{1}{2} \partial_\mu \chi \partial^\mu \chi - \frac{1}{2} m_\chi^2 \chi^2 - \frac{5}{6} \frac{m_\chi^2}{f_d^2} \chi^3 + \frac{1}{2f_d^2} \partial_\mu \pi \partial^\mu \pi \chi^2 + \dots \end{aligned} \quad (4)$$

where  $m_\chi^2 = \frac{\partial^2 V(\chi)}{\partial \chi^2} \Big|_{\chi=f_d}$ .

At very low temperatures, i.e.,  $\beta \rightarrow \infty$ , bosonic contributions to one-loop order are suppressed by  $O(\frac{1}{\beta})$  or  $O(e^{-\beta m_\chi})$ . This can be seen without evaluations of the diagrams. At low temperature, the Bose-Einstein distribution function  $n_B(k) = \frac{1}{e^{\beta k} - 1}$  goes to zero but the Fermi-Dirac distribution function  $n_F(p) = \frac{1}{e^{\beta(p-\mu)} + 1}$  becomes  $\theta(\mu - p)$ . Thus in our case, the finite-temperature and -density corrections come from quark propagators.

In our calculations of Feynman integrals, we shall follow the method of Niemi and Semenoff [11]. In the case of renormalization of finite-temperature

---

<sup>2</sup>Since the role of gluons in the constituent quark model is negligible, we will ignore the terms containing gluons[10].

QED [12] one encounters a new singularity like  $\frac{1}{k} \frac{1}{e^{\beta k} - 1}$ . However in our case, because pion-quark vertices depend on momentum, we do not have any additional infrared singularities at finite temperature and density. At finite temperature and density, the lack of explicit Lorentz invariance causes some ambiguities in defining mass corrections. The standard practice is to define  $\rho$ -dependent (or  $T$ -dependent) mass corrections as the energy of the particle at  $\vec{p} = 0$  [13]. In our case, this definition may not be the most suitable one because of the Fermi blocking from the fermions inside the Fermi sphere. We find it simplest and most convenient to define the mass at  $\vec{p} = 0$ .

### 3 Pion mass

We first consider pion mass at low temperature and high density. There are three density-dependent diagrams Fig. 1 that may contribute to pion mass corrections. The first one, Fig. 1a, vanishes identically due to isospin symmetry. Explicit calculation of the two diagrams in Fig. 1b gives, for  $\beta \rightarrow \infty$ ,

$$\begin{aligned}
-i\Sigma_\pi(p^2) &= \left(\frac{g_A}{f_\pi}\right)^2 \text{tr} \int \frac{d^4k}{(2\pi)^4} \not{p}\gamma_5 T^a (\not{p} + \not{k} + m) \cdot \not{p}\gamma_5 T^a (\not{k} + m) \\
&\quad \left[ \frac{i}{(p+k)^2 - m^2} (-2\pi) \delta(k^2 - m^2) \sin^2 \theta_{k_0} \right. \\
&\quad \left. + \frac{i}{k^2 - m^2} (-2\pi) \delta((k+p)^2 - m^2) \sin^2 \theta_{k_0+p_0} \right] \\
&= 2i \left(\frac{g_A}{f_\pi}\right)^2 \int \frac{d^4k}{(2\pi)^3} (p \cdot k (p^2 + 2k \cdot p) - 2m^2 p^2) \\
&\quad \times \left[ \frac{1}{(p+k)^2 - m^2} 2\pi \delta(k^2 - m^2) \sin^2 \theta_{k_0} \right. \\
&\quad \left. + \frac{1}{k^2 - m^2} 2\pi \delta((k+p)^2 - m^2) \sin^2 \theta_{k_0+p_0} \right]. \tag{5}
\end{aligned}$$

With the change of variable on the second term,  $p+k \rightarrow k$ , the above integral can be rewritten as

$$\Sigma_\pi(p^2) = -2 \left(\frac{g_A}{f_\pi}\right)^2 \int \frac{d^4k}{(2\pi)^3} \left[ \frac{-p \cdot k (p^2 + 2k \cdot p) + 2m^2 p^2}{p^2 + 2k \cdot p} \right]$$

$$\begin{aligned}
& + \frac{p \cdot k(p^2 - 2k \cdot p) + 2m^2 p^2}{p^2 - 2k \cdot p}] \delta(k^2 - m^2) \sin^2 \theta_{k_0} \\
= & -2p^2 \left(\frac{g_A}{f_\pi}\right)^2 \int \frac{d^4 k}{(2\pi)^3} \left[ \frac{2m^2}{p^2 + 2k \cdot p} + \frac{2m^2}{p^2 - 2k \cdot p} \right] \\
& \times \delta(k^2 - m^2) \sin^2 \theta_{k_0}. \tag{6}
\end{aligned}$$

Since the pion self-energy is proportional to  $p^2$ , the pole of the pion propagator does not change. Hence the pion remains massless as long as there is no explicit chiral symmetry breaking. Naively we might expect that the pion may acquire a dynamical mass due to dynamical screening from thermal particles or particle density, which is the case for QED [14] even with gauge invariance. The reason for this is the derivative pion coupling to the quark field. In eq.(5), the terms with  $p \cdot k$  may give rise terms not proportional to  $p^2$ , which lead to the pion mass correction after  $dk$  integration. However, those terms are proportional to  $p^2 + 2k \cdot p$  or  $p^2 - 2k \cdot p$  which are cancelled by the their denominators and contribute nothing after the  $dk$  integration. This feature has been explicitly demonstrated from eq.(5) to eq.(6).

In our previous work using the dilated chiral quark model [8], where effective potential method was used, there were seven diagrams contributing to the pion self-energy at finite temperature. Those diagrams cancel among themselves to leave the pion massless.

After spatial momentum integration, we get

$$\begin{aligned}
\Sigma_\pi(p^2) &= -2 \left(\frac{g_A}{f_\pi}\right)^2 \frac{m^2 p^2}{4\pi^2} \int dk_0 dx \bar{k} \left[ \frac{1}{p^2 + 2Ek_0 - 2\bar{k}\bar{p}x} + \frac{1}{p^2 - 2Ek_0 + 2\bar{k}\bar{p}x} \right] \sin^2 \theta_{k_0} \\
&= \left(\frac{g_A}{f_\pi}\right)^2 \frac{m^2 p^2}{4\pi^2} \int dk_0 \bar{k} \frac{1}{\bar{k}\bar{p}} \left( \ln \left| \frac{p^2 + 2Ek_0 - 2\bar{k}\bar{p}}{p^2 + 2Ek_0 + 2\bar{k}\bar{p}} \right| \right. \\
&\quad \left. - \ln \left| \frac{p^2 - 2Ek_0 + 2\bar{k}\bar{p}}{p^2 - 2Ek_0 - 2\bar{k}\bar{p}} \right| \right) \sin^2 \theta_{k_0} \tag{7}
\end{aligned}$$

where we used  $\vec{k} \cdot \vec{p} = \bar{p}\bar{k}x$  and  $E \equiv p_0$ . Since the pole of the pion propagator does not change, we can take the renormalization point at  $p^2 = 0$ . Then the integrand itself vanishes, so there is no wave-function renormalization for the pion in dense medium.

## 4 Quark mass

At one-loop order, the quark self-energy is given by the diagrams of Fig. 2 and Fig. 3. The diagram Fig. 2 gives

$$\begin{aligned}
-i\Sigma_Q^{(1)}(p) &= \left(-i\frac{m}{f_d}\right)^2 \frac{i}{-m_\chi^2} \rho_s \\
&= i\left(\frac{m}{f_d}\right)^2 \frac{\rho_s}{m_\chi^2}
\end{aligned} \tag{8}$$

where  $\rho_s$  is the scalar density obtained from the fermionic loop with thermal propagator,

$$\begin{aligned}
\rho_s &= -tr \int \frac{d^4p}{(2\pi)^4} (-2\pi)(\not{p} + m)\delta(p^2 - m^2)\sin^2\theta_{p_0} \\
&= 4 \int \frac{d^3\vec{p}}{(2\pi)^3} dp_0 \frac{m}{\sqrt{\vec{p}^2 + m^2}} \delta(p_0 - \sqrt{\vec{p}^2 + m^2})\theta(\mu - p_0) \\
&= 4\theta(\mu - m) \int_0^{\vec{p}_F} \frac{d^3\vec{p}}{(2\pi)^3} \frac{m}{\sqrt{\vec{p}^2 + m^2}} \\
&= \frac{m}{\pi^2} \theta(\mu - m) [\mu\sqrt{\mu^2 - m^2} - m^2 \ln\left(\frac{\mu + \sqrt{\mu^2 - m^2}}{m}\right)]
\end{aligned} \tag{9}$$

where  $\vec{p}_F^2 = \mu^2 - m^2$ . With  $I$  defined as

$$I = \frac{1}{4\pi^2} \theta(\mu - m) [\mu\sqrt{\mu^2 - m^2} - m^2 \ln\left(\frac{\mu + \sqrt{\mu^2 - m^2}}{m}\right)] \tag{10}$$

we get

$$\rho_s = 4mI \tag{11}$$

$$\Sigma_Q^{(1)}(p) = -\left(\frac{m}{f_d}\right)^2 \frac{4m}{m_\chi^2} I \tag{12}$$

The radiative correction from the pion field in Fig. 3a is

$$\begin{aligned}
-i\Sigma_Q^{3a}(p) &= -\left(\frac{g_A}{f_\pi}\right)^2 \int \frac{d^4q}{(2\pi)^4} \frac{i}{(p-q)^2} (\not{p}-\not{q})\gamma_5 T^a \\
&\quad \times (-2\pi)\delta(q^2 - m^2)(\not{q} + m)(\not{p}-\not{q})\gamma_5 T^a \sin^2\theta_{q_0} \\
&= -i\frac{3}{8}\left(\frac{g_A}{f_\pi}\right)^2 [(\not{p} + m)I].
\end{aligned} \tag{13}$$

(The details of the calculation are given in Appendix II.)

Finally, the radiative correction due to the scalar in Fig. 3b is found to be

$$\begin{aligned}
-i\Sigma_Q^{3b}(p) &= i\left(\frac{m}{f_d}\right)^2 \int \frac{d^4k}{(2\pi)^3} \frac{\not{k} + m}{2m^2 - 2p \cdot k - m_\chi^2} \delta(k^2 - m^2) \sin^2 \theta_{k_0} \\
&= i\left(\frac{m}{f_d}\right)^2 \left[ \mathcal{J} - \frac{m}{2m_\chi^2} I \right]
\end{aligned} \tag{14}$$

where  $\mathcal{J}$  is

$$\mathcal{J} \equiv \int \frac{d^4k}{(2\pi)^3} \frac{\not{k}}{2m^2 - 2p \cdot k - m_\chi^2} \delta(k^2 - m^2) \sin^2 \theta_{k_0}. \tag{15}$$

In sum, the self-energy of the quark with four momentum  $(E, \vec{p})$  can be written in the form

$$\Sigma_Q(E, \vec{p}) = aE\gamma_0 + b\vec{\gamma} \cdot \vec{p} + c \tag{16}$$

where  $a$ ,  $b$ , and  $c$  are

$$\begin{aligned}
a &= \frac{3}{8} \left(\frac{g_A}{f_\pi}\right)^2 I - \frac{1}{E} \left(\frac{m}{f_d}\right)^2 J^0 \\
b &= -\frac{3}{8} \left(\frac{g_A}{f_\pi}\right)^2 I + \left(\frac{m}{f_d}\right)^2 \frac{1}{\vec{p}^2} \vec{J} \cdot \vec{p} \\
c &= -\left(\frac{m}{f_d}\right)^2 \frac{4m}{m_\chi^2} I + \frac{3}{8} \left(\frac{g_A}{f_\pi}\right)^2 m I + \left(\frac{m}{f_d}\right)^2 \frac{m}{2m_\chi^2} I
\end{aligned} \tag{17}$$

where we have used the relation [12],

$$\vec{J} \cdot \vec{\gamma} = \frac{\vec{J} \cdot \vec{p} \vec{p} \cdot \vec{\gamma}}{\vec{p}^2}. \tag{18}$$

From eq.(17), we can see that the scalar field radiative correction violates the Lorentz symmetry, that is,  $a \neq -b$ , unless  $\frac{1}{E} J^0 = \frac{1}{\vec{p}^2} \vec{J} \cdot \vec{p}$ . On the other hand, the pion radiative corrections in  $a$  and  $b$  preserve Lorentz covariance. Since we have only  $O(3)$  symmetry in the medium for the quark propagation, we will adopt the conventional definition of mass as a zero of the inverse propagator with zero momentum. The inverse propagator of the quark is given by

$$G^{-1}(E, p) = \not{p} - m - \Sigma(E, \vec{p}) \tag{19}$$

$$= E(1 - a)\gamma_0 - (1 + b)\vec{\gamma} \cdot \vec{p} - c - m \tag{20}$$

The mass is now defined as the energy which satisfies  $\det(G^{-1}) = 0$  with  $\vec{p}^2 = 0$ ,

$$(1 - a)E = c + m. \quad (21)$$

Since  $a$  and  $c$  are perturbative corrections, eq.(21) can be approximated to the leading order as

$$E = m + c + ma. \quad (22)$$

Then the quark mass identified as  $E$  in eq.(22) is

$$\begin{aligned} m_{phys} &= m - \left(\frac{m}{f_d}\right)^2 \frac{4m}{m_\chi^2} I \\ &\quad + \frac{3}{4} \left(\frac{g_A}{f_\pi}\right)^2 m I \\ &\quad - \left(\frac{m}{f_d}\right)^2 J^0 + \left(\frac{m}{f_d}\right)^2 \frac{m}{2m_\chi^2} I. \end{aligned} \quad (23)$$

The first line in eq.(23) is just the result of the mean-field approximation, in which only the tadpole diagram, Fig. 1, is taken into account, as further elaborated on in the next section. While the dropping of the quark mass with density is obvious in the mean-field approximation, it is not clear whether it is still true when the radiative corrections are included as in the second and the third lines in eq.(23).

We evaluate  $J^0$  in two extreme limits. In the limit of large scalar mass,  $m_\chi^2 \gg \mu^2 > m^2 \sim E_Q^2$ , we get

$$J^0 = -\frac{1}{12\pi^2} \frac{1}{m_\chi^2} (\mu^2 - m^2)^{3/2}. \quad (24)$$

The details of the evaluation up to order of  $\frac{m^2}{m_\chi^2}$ ,  $\frac{\mu^2}{m_\chi^2}$  and  $\frac{E^2}{m_\chi^2}$  are given in Appendix II.

In the extreme relativistic limit of the quark<sup>3</sup>, the contributions from the scalar become negligible in  $a$  and  $b$  as can be seen in eq.(17) and we recover Lorentz covariance as expected. The quark mass in this case is given by

$$m_{phys} = m - \left(\frac{m}{f_d}\right)^2 \frac{4m}{m_\chi^2} I$$

---

<sup>3</sup>One can imagine that the probing quark inside the medium can be highly relativistic.

$$\begin{aligned}
& + \frac{3}{4} \left( \frac{g_A}{f_\pi} \right)^2 m I \\
& + \left( \frac{m}{f_d} \right)^2 \frac{m}{2m_\chi^2} I.
\end{aligned} \tag{25}$$

Again the effect of radiative corrections in the medium is opposite to that of mean-field approximation (tadpole diagram).

The result obtained at the one-loop order does not indicate in an unambiguous way that the quark mass is scaling in medium according to BR scaling [1]. The specific behavior depends on the strength of the coupling constants involved in the theory,  $g_A, m, f_\pi$  and the VEV  $f_d$ . This does not seem to be the correct physics for BR scaling as evidenced in Nature. We suggest that counting should be organized in terms of  $1/N_c$  where  $N_c$  is the number of colors. Then all the radiative corrections involving quark loops in the QCD variables must be suppressed by a factor of  $\frac{1}{N_c}$  compared to the tadpole diagram. In the large  $N_c$  and/or high energy/momentum limit, the quark propagator retains Lorentz covariance and the mass does decrease according to the mean-field approximation.

## 5 *Scalar mass*

Now consider the mass shift of the scalar  $\chi$ -field (see Fig. 4 and Fig. 5). The tadpole diagram, Fig. 4, gives

$$\begin{aligned}
-i\Sigma_\chi^{(2)}(p) &= -\frac{5}{6} \frac{m_\chi^2}{f_d} \left( -i \frac{m}{f_d} \right) \rho_s \left( \frac{i}{-m_\chi^2} \right) 3! = 5i \frac{m}{f_d^2} \rho_s \\
&= i20 \left( \frac{m}{f_d} \right)^2 I
\end{aligned} \tag{26}$$

where the factor  $3!$  comes from the topology of the diagram. This corresponds to the mean-field approximation.

Now consider Fig. 5. It is calculated to be

$$\begin{aligned}
-i\Sigma_\chi^{(5)}(p) &= -i \frac{m^2}{m_\chi^2} \frac{8}{\pi^2} \left( \frac{m}{f_d} \right)^2 \left[ \frac{1}{2} \theta(\mu - m) (\mu \sqrt{\mu^2 - m^2} - m^2 \ln \left( \frac{\mu + \sqrt{\mu^2 - m^2}}{m} \right)) \right. \\
&\quad \left. - \frac{E^2}{m_\chi^2} \left( \frac{\mu(\mu^2 - m^2)^{3/2}}{4m^2} + \frac{\mu \sqrt{\mu^2 - m^2}}{8} \right) \right]
\end{aligned}$$

$$-\frac{m^2}{8} \ln\left(\frac{\mu + \sqrt{\mu^2 - m^2}}{m}\right) \Big]. \quad (27)$$

Note that the terms on the second and the third lines contribute only to the *energy* of the  $\chi$ -field and hence break Lorentz invariance. We can sum up the above results to get

$$\begin{aligned} \delta m_\chi^2 = & \left(\frac{m}{f_d}\right)^2 \left[ -\frac{5}{\pi^2} \theta(\mu - m) (\mu \sqrt{\mu^2 - m^2} - m^2 \ln\left(\frac{\mu + \sqrt{\mu^2 - m^2}}{m}\right)) \right. \\ & + \frac{8}{\pi^2} \left( \frac{1}{2} \frac{m^2}{m_\chi^2} \theta(\mu - m) (\mu \sqrt{\mu^2 - m^2} - m^2 \ln\left(\frac{\mu + \sqrt{\mu^2 - m^2}}{m}\right)) \right. \\ & - \frac{E^2}{m_\chi^2} \left( \frac{\mu(\mu^2 - m^2)^{3/2}}{4m_\chi^2} + \frac{m^2 \mu \sqrt{\mu^2 - m^2}}{m_\chi^2 8} \right) \\ & \left. \left. - \frac{m^2}{m_\chi^2} \frac{m^2}{8} \ln\left(\frac{\mu + \sqrt{\mu^2 - m^2}}{m}\right) \right) \right] \end{aligned} \quad (28)$$

For large scalar mass, we can neglect the second term because it is much smaller than the first one due to the factors,  $\frac{m^2}{m_\chi^2}$  and  $\frac{\mu^2}{m_\chi^2}$ .

$$\delta m_\chi^2 \cong \left(\frac{m}{f_d}\right)^2 \left[ -\frac{5}{\pi^2} \theta(\mu - m) (\mu \sqrt{\mu^2 - m^2} - m^2 \ln\left(\frac{\mu + \sqrt{\mu^2 - m^2}}{m}\right)) \right] \quad (29)$$

The physical  $\chi$ -mass becomes

$$m_{\chi^{phys}}^2 = m_\chi^2 - 20 \left(\frac{m}{f_d}\right)^2 I. \quad (30)$$

We see that Lorentz invariance is maintained. The mass of the  $\chi$  field drops as density increases. This is consistent with the tendency for the scalar to become dilatonic at large density, providing an answer to the question posed at the beginning.

As in the case of the quark mass corrections, we should check that the terms that break Lorentz invariance do become negligible at high energy and momentum. For this, we recalculate Fig. 5 at high energy and momentum ( $\bar{p} \simeq E$ ,  $p^2 \simeq 0$ )

$$-i\Sigma_\chi^{(5)}(p) = -i\left(\frac{m}{f_d}\right)^2 \frac{1}{\pi^2} \int dq_0 \bar{q} \left[ 2 + \frac{p^2 - 4m^2}{4\bar{p}^2 q^2} \ln\left(\frac{p^2 + 2E q_0 - 2\bar{p}\bar{q}}{p^2 + 2E q_0 + 2\bar{p}\bar{q}}\right) \right]$$

$$\begin{aligned}
& -\frac{p^2 - 4m^2}{4\bar{p}^2 q^2} \ln\left(\frac{p^2 + 2E q_0 - 2\bar{p}\bar{q}}{p^2 + 2E q_0 + 2\bar{p}\bar{q}}\right)] \\
\simeq & -i\left(\frac{m}{f_d}\right)^2 \frac{1}{\pi^2} \int dq_0 \bar{q} \left[ 2 + \frac{1}{\bar{p}^2} \frac{p^2 - 4m^2}{4q^2} \ln\left(\frac{q_0 - \bar{q}}{q_0 + \bar{q}}\right) \right. \\
& \left. - \frac{1}{\bar{p}^2} \frac{p^2 - 4m^2}{4q^2} \ln\left(\frac{q_0 - \bar{q}}{q_0 + \bar{q}}\right) \right] \\
= & -i\left(\frac{m}{f_d}\right)^2 \frac{1}{\pi^2} \int dq_0 2\bar{q} \\
= & -i\left(\frac{m}{f_d}\right)^2 \frac{1}{\pi^2} \theta(\mu - m) \left[ \mu \sqrt{\mu^2 - m^2} - m^2 \ln\left(\frac{\mu + \sqrt{\mu^2 - m^2}}{m}\right) \right]
\end{aligned} \tag{31}$$

This does not violate Lorentz covariance since it has no energy or momentum dependences. From eqs.(26) and (31), the physical mass of the  $\chi$  becomes

$$m_{\chi^{phys}}^2 = m_\chi^2 - 16\left(\frac{m}{f_d}\right)^2 I. \tag{32}$$

## 6 Mean-Field Approach

So far, we have not taken into account the fact that introducing the thermal fluctuation can cause further shifting of the vacuum expectation value of the  $\chi$ -field.

The introduction of the thermal vacuum,  $|0(\beta)\rangle$ , implies the necessity of shifting the vacuum expectation value of  $\chi$ . We will therefore impose the condition that all tadpole graphs vanish on the physical vacuum (see Appendix C of ref.[15]). In terms of Weinberg's notation, the condition is

$$\left(\frac{\partial P(\pi)}{\partial \phi}\right)_{\phi=\langle\phi\rangle_0} + \tilde{T} = 0 \tag{33}$$

where  $P(\phi)$  is a polynomial in  $\phi$  and  $\tilde{T}$  is the sum of tadpole graphs. We have inserted the factor  $-i(2\pi)^4$  into  $\tilde{T}$ . In our case, the above condition reads

$$-m_\chi^2 \chi_0 - \frac{m}{f_d} \rho_s = 0 \tag{34}$$

where we have dropped higher powers of the  $\chi$ -field and retained only the tadpoles that depend on density at one-loop order. From eq.(34), we get the

vacuum expectation value of the  $\chi$ -field

$$\langle 0|\chi|0 \rangle \equiv \chi_0 = -\frac{m}{m_\chi^2 f_d} \rho_s. \quad (35)$$

This is equivalent to Fig. 1 without the external quark line. With the shift of the  $\chi$ -field around  $\chi_0$ , i.e.,  $\chi \rightarrow \chi_0 + \chi$ , the Lagrangian is modified to

$$\begin{aligned} L &= \bar{\psi}i(\not{\partial} + \not{Y})\psi + g_A \bar{\psi} A \gamma_5 \psi - (m + \frac{m}{f_d} \chi_0) \bar{\psi} \psi - \frac{m}{f_d} \bar{\psi} \psi \chi \\ &+ \frac{1}{4} \frac{f_\pi^2}{f_d^2} \text{tr}(\partial_\mu U \partial^\mu U^\dagger) \chi^2 + \frac{1}{4} \frac{f_\pi^2}{f_d^2} (f_d + \chi_0)^2 \text{tr}(\partial_\mu U \partial^\mu U^\dagger) \\ &+ \frac{1}{2} \partial_\mu \chi \partial^\mu \chi - V(f_d + \chi_0 + \chi) + \dots \end{aligned} \quad (36)$$

where  $U = e^{i\frac{\pi^*}{f_\pi^*}}$ .<sup>4</sup> We will hereafter replace  $\pi^*$  by  $\pi$ . The Lagrangian (36) shows explicitly the density dependence of  $f_\pi$  and  $m_\chi^2$ :

$$\begin{aligned} f_\pi^{*2} &= f_\pi^2 \left(1 + \frac{\chi_0}{f_d}\right)^2 = f_\pi^2 \left(1 + 2\frac{\chi_0}{f_d}\right) \\ m_\chi^{*2} &= \frac{\partial^2 V(\chi)}{\partial \chi^2} \Big|_{\chi=f_d+\chi_0} = \frac{m_\chi^2}{f_d^2} (f_d + \chi_0)^2 \left[1 + 3 \ln\left(1 + \frac{\chi_0}{f_d}\right)\right] \\ &\simeq m_\chi^2 \left(1 + \frac{\chi_0}{f_d}\right)^2 \left(1 + 3\frac{\chi_0}{f_d}\right) \simeq m_\chi^2 \left(1 + 5\frac{\chi_0}{f_d}\right) \\ m^{*2} &= m^2 \left(1 + \frac{\chi_0}{f_d}\right)^2 = m^2 \left(1 + 2\frac{\chi_0}{f_d}\right). \end{aligned} \quad (37)$$

Note that  $\chi_0$  is negative. We conclude that the effect of one-loop tadpole diagrams follows the scaling

$$\frac{m^*}{m} = \frac{f_\pi^*}{f_\pi} \simeq \frac{m_\chi^*}{m_\chi}. \quad (38)$$

To make a complete mass correction at one-loop order, we need to incorporate the corrections from Fig. 3 and Fig. 5 into the Lagrangian. However in the present case, we need not include Figs. 2 and 4: they are already included in the shifting of the vacuum expectation value. Incorporation of

---

<sup>4</sup>Our  $f_d + \chi_0$  corresponds to  $\chi^*$  in ref[1].

the corrections from Figs. 3 and 5 into our Lagrangian brings in Lorentz non-invariant terms in the fermionic sector as observed in the previous section. In the bosonic sector, Lorentz symmetry is preserved and the mean-field approximation is approximately valid. In the Large  $N_c$  limit, the mean-field approximation is the leading order in the quark mass corrections in the medium.

## 7 *Discussion*

The aim of the paper was to see whether a perturbative calculation starting from a chiral Lagrangian implemented with the QCD trace anomaly could lead, in the presence of nuclear matter, to the dilated chiral quark model that exhibits Weinberg's mended symmetry *and* BR scaling. We found that in the large  $N_c$  limit (and large scalar mass limit), the tadpoles dominate and hence the mean-field approximation is reliable, giving rise a Lorentz-invariant Lagrangian with the masses scaling according to BR scaling. However for finite  $N_c$ , loop corrections are not negligible and behave counter to the tadpole contributions. Radiative corrections bring Lorentz-symmetry-breaking terms invalidating the assumption made in [8] except when the quark or scalar particle probed is of high energy. In the chiral limit, the pion remains massless and its behavior in medium Lorentz symmetric.

The conclusion that emerges from this calculation is that the dilated chiral quark model can emerge in dense and hot medium – if it does at all – only through nonperturbative processes (e.g., large  $N_c$  expansion) starting from a chiral Lagrangian. This issue will be addressed in a future publication.

### **Acknowledgments**

We thank Professor M. Rho for suggestions and discussions about the main content of this paper. This work was supported in part by the Korea Ministry of Education (BSRI-95-2441) and in part by the Korea Science and Engineering Foundation under Grants No. 94-0702-04-01-3

## **References**

- [1] G.E. Brown and M. Rho, Phys. Rev. Lett. **66**, 2720 (1991)
- [2] G.E. Brown and M. Rho, Phys. Rep. **269**, 333 (1996)
- [3] G.Q. Li, C.M. Ko and G.E. Brown, Phys. Rev. Lett. **75**, 4007 (1996); Nucl. Phys., in press and papers in preparation.
- [4] B. Friman and M. Rho, Phys. Repts., in press and nucl-th/96022025; M. Rho, KOSEF Lecture, February 1996, Seoul, Korea; “QCD vacuum changes in nuclei,” talk at the International Symposium on Non-Nucleonic Degrees of Freedom Detected in Nucleus, 2-5 September 1996, Osaka, Japan.
- [5] S. Beane and U. van Kolck, Phys. Lett. **B328**, 137 (1994)
- [6] S. Weinberg, Phys. Rev. Lett. **65**, 1177 (1990)
- [7] G.E. Brown, M. Buballa and M. Rho, Nucl. Phys., in press.
- [8] Y. Kim, H. K. Lee and M. Rho, Phys. Rev. **C52**, R1184 (1995)
- [9] P. Braun-Munzinger and J. Stachel, nucl-th/9606017
- [10] A. Manohar and H. Georgi, Nucl. Phys. **B234**, 189 (1984)
- [11] A. J. Niemi and G. W. Semenoff, Nucl. Phys. **B230**[FS10], 181 (1984)
- [12] J.F. Donoghue and B.R. Holstein, Phys. Rev. **D28**, 340 (1983)
- [13] J.-P. Blaizot, JKPS **25**, S65 (1992)
- [14] S. S. Masood, Phys. Rev. **D44**, 3943 (1991)
- [15] S. Weinberg, Phys. Rev. **D7**, 2887 (1973)
- [16] H. Matsumoto in *Progress in Quantum Field Theory*, ed. by H. Ezawa and S. Kamefuchi (North-Holland, Amsterdam, 1986)
- [17] K. Saito, T. Maruyama and K. Soutome, Phys. Rev. **C40**, 407 (1989)

## Appendix I

We summarize the basic notation and definition of Thermo Field Dynamics(TFD) [16][17]. TFD is a real time operator formalism in quantum field theory at finite temperature. The main feature of the TFD is that thermal average of operator  $A$  is defined as the expectation value with respect to the temperature dependent vacuum,  $|0(\beta)\rangle$ , which is introduced through Bogoliubov transformation.

$$\begin{aligned} \langle A \rangle &\equiv \text{Tr}(Ae^{-\beta(H-\mu)})/\text{Tr}(e^{-\beta(H-\mu)}) \\ &= \langle 0(\beta) | A | 0(\beta) \rangle \end{aligned} \quad (39)$$

where  $\beta \equiv \frac{1}{kT}$ ,  $H$  is the total Hamiltonian of the system, and  $\mu$  is the chemical potential. The propagator in TFD can be separated into two parts, i.e., the usual Feynmann part  $G_F$  and density-dependent part  $G_D$ ,

$$G_{\alpha\beta} = G_{F\alpha\beta} + G_{D\alpha\beta}. \quad (40)$$

For fermion with mass  $m$ ,

$$\begin{aligned} G_{F\alpha\beta} &= (\not{p} + m)_{\alpha\beta} \begin{pmatrix} \frac{1}{p^2 - m^2 + i\epsilon} & 0 \\ 0 & \frac{1}{p^2 - m^2 - i\epsilon} \end{pmatrix} \\ G_{D\alpha\beta} &= 2\pi i \delta(p^2 - m^2) (\not{p} + m)_{\alpha\beta} \begin{pmatrix} \sin^2 \theta_{p_0} & \frac{1}{2} \sin 2\theta_{p_0} \\ \frac{1}{2} \sin 2\theta_{p_0} & -\sin^2 \theta_{p_0} \end{pmatrix} \end{aligned} \quad (41)$$

with

$$\begin{aligned} \cos \theta_{p_0} &= \frac{\theta(p_0)}{(1 + e^{-x})^{1/2}} + \frac{\theta(-p_0)}{(1 + e^x)^{1/2}}, \\ \sin \theta_{p_0} &= \frac{e^{-x/2}\theta(p_0)}{(1 + e^{-x})^{1/2}} - \frac{e^{x/2}\theta(-p_0)}{(1 + e^x)^{1/2}}, \end{aligned} \quad (42)$$

where  $\alpha$  and  $\beta$  are Dirac indices and  $x = \beta(p_0 - \mu)$ .

The propagator of the scalar particle with mass  $m_s$  is given by

$$\Delta(p) = \Delta_F(p) + \Delta_D(p), \quad (43)$$

where

$$\begin{aligned} \Delta_F &= \begin{pmatrix} \frac{1}{p^2 - m_s^2 + i\epsilon} & 0 \\ 0 & \frac{-1}{p^2 - m_s^2 - i\epsilon} \end{pmatrix} \\ \Delta_D &= -2\pi i \delta(p^2 - m_s^2) \begin{pmatrix} \sinh^2 \phi_{p_0} & \frac{1}{2} \sinh 2\phi_{p_0} \\ \frac{1}{2} \sinh 2\phi_{p_0} & \sinh^2 \phi_{p_0} \end{pmatrix} \end{aligned} \quad (44)$$

with

$$\begin{aligned}\cosh \phi_{p_0} &= \frac{1}{(1 - e^{-|y|})^{1/2}}, \\ \sinh \phi_{p_0} &= \frac{e^{-|y|/2}}{(1 - e^{-|y|})^{1/2}},\end{aligned}\tag{45}$$

where  $y = \beta p_0$ .

## Appendix II

In this Appendix II, we will evaluate various intergrals in the text.

1. The contribution for the quark self energy from Fig. 3a(pion radiative corrections) is given by

$$\begin{aligned}
-i\Sigma_Q^{3a}(p) &= -\left(\frac{g_A}{f_\pi}\right)^2 \int \frac{d^4k}{(2\pi)^4} \frac{i}{(p-k)^2} (\not{p}-\not{k})\gamma_5 T^a \\
&\quad \times (-2\pi)\delta(k^2-m^2)(\not{k}+m)(\not{p}-\not{k})\gamma_5 T^a \sin^2\theta_{k_0} \\
&= i\frac{3}{4}\left(\frac{g_A}{f_\pi}\right)^2 \int \frac{d^4k}{(2\pi)^3} \frac{-(p-k)^2 \not{k} + 2(p-k)\cdot k(\not{p}-\not{k}) - m(p-k)^2}{(p-k)^2} \\
&\quad \times \delta(k^2-m^2) \sin^2\theta_{k_0} \\
&= i\frac{3}{4}\left(\frac{g_A}{f_\pi}\right)^2 \int \frac{d^4k}{(2\pi)^3} [-\not{k} - (\not{p}-\not{k}) - m]\delta(k^2-m^2) \sin^2\theta_{k_0} \\
&= -i\frac{3}{4}\left(\frac{g_A}{f_\pi}\right)^2 (\not{p}+m) \frac{1}{4\pi^2} \int dk_0 \bar{k} \sin^2\theta_{k_0} \\
&= -i\frac{3}{8\pi^2}\left(\frac{g_A}{f_\pi}\right)^2 (\not{p}+m)I
\end{aligned} \tag{46}$$

where  $\bar{k}$  denotes  $|\vec{k}|$ . This gives eq.(13) in section 4.

$I$ , eq.(10) in the text, is defined in the low temperature limit as in ref.[11],

$$\begin{aligned}
I &= \int \frac{dk_0}{2\pi^2} \sqrt{k_0^2 - m^2} \sin^2\theta_{k_0} \\
&= \int \frac{dk_0}{2\pi^2} \sqrt{k_0^2 - m^2} \theta(\mu - m) \\
&= \frac{1}{4\pi^2} \theta(\mu - m) \cdot (\mu\sqrt{\mu^2 - m^2} - m^2 \ln(\frac{\mu + \sqrt{\mu^2 - m^2}}{m}))
\end{aligned} \tag{47}$$

where we have used the fact that  $\frac{1}{1+\exp[\beta(k_0-\mu)]}|_{\beta\rightarrow\infty} \rightarrow \theta(\mu - k_0)$ .

2. We evaluate  $J^0$  and  $\vec{J}\cdot\vec{p}$  defined in eq.(15), which are needed in the evaluation of the quark mass correction from  $\chi$ -field in Fig. 3b. Firstly let us consider  $J^0$ ,

$$\begin{aligned}
J^0 &= \int \frac{d^4k}{(2\pi)^3} \frac{k_0}{2m^2 - 2p\cdot k - m_\chi^2} \delta(k^2 - m^2) \sin^2\theta_{k_0} \\
&= \int \frac{d^3\vec{k}}{(2\pi)^3} \frac{1}{2} \frac{1}{2m^2 - 2p\cdot k - m_\chi^2} \sin^2\theta_{k_0}
\end{aligned} \tag{48}$$

Note that due to the factor  $\sin^2 \theta_{k_0} |_{\beta \rightarrow \infty} \rightarrow \theta(\mu - k_0)$ ,  $k$  is maximally order of chemical potential, i.e.,  $k \sim \mu$ . Assuming large dilaton mass,  $m_\chi^2 \gg \mu^2 > m^2 \sim E_Q^2$ ,

$$\begin{aligned}
J^0 &= \int \frac{d^3 \vec{k}}{(2\pi)^3} \frac{1}{2} \frac{1}{2m^2 - 2p \cdot k - m_\chi^2} \sin^2 \theta_{k_0} \\
&= \frac{1}{8\pi^2} \int_0^{k_F} d\bar{k} \bar{k}^2 \frac{1}{2\bar{p}\bar{k}} \ln\left(\frac{2\bar{p}\bar{k} + 2m^2 - 2Ek_0 - m_\chi^2}{-2\bar{p}\bar{k} + 2m^2 - 2Ek_0 - m_\chi^2}\right) \\
&\cong -\frac{1}{4m_\chi^2 \pi^2} \int_0^{k_F} d\bar{k} \bar{k}^2 \\
&= -\frac{1}{12\pi^2} \frac{1}{m_\chi^2} (\mu^2 - m^2)^{3/2}
\end{aligned} \tag{49}$$

where we discarded the terms with higher power of  $\frac{Ek_F}{m_\chi^2}$  or  $\frac{m^2}{m_\chi^2}$ .

Similarly,

$$\vec{J} \cdot \vec{p} = \int \frac{d^4 k}{(2\pi)^3} \frac{\vec{p} \cdot \vec{k}}{2m^2 - 2p \cdot k - m_\chi^2} \delta(k^2 - m^2) \sin^2 \theta_{k_0} \tag{50}$$

can be approximated

$$\begin{aligned}
\vec{J} \cdot \vec{p} &= \frac{1}{8\pi^2} \int dk_0 \bar{k} \left[ 1 - \frac{2m^2 - m_\chi^2 - 2Ek_0}{4\bar{p}\bar{k}} \ln\left(\frac{2\bar{p}\bar{k} + 2m^2 - 2Ek_0 - m_\chi^2}{-2\bar{p}\bar{k} + 2m^2 - 2Ek_0 - m_\chi^2}\right) \right] \\
&\cong \frac{1}{8\pi^2} \frac{4E^2}{m_\chi^4} \int dk_0 k_0^2 \bar{k} \\
&= \frac{1}{8\pi^2} \frac{E^2}{m_\chi^4} \theta(\mu - m) [\mu(\mu^2 - m^2)^{3/2} \\
&\quad + \frac{m^2 \mu \sqrt{\mu^2 - m^2}}{2} - \frac{m^4}{2} \ln\left(\frac{\mu + \sqrt{\mu^2 - m^2}}{m}\right)]
\end{aligned} \tag{51}$$

**3.** The contribution from Fig. 5 for the  $\chi$  self energy, eq.(26), is given by

$$\begin{aligned}
-i\Sigma_\chi^{(5)}(p^2) &= -\left(\frac{m}{f_d}\right)^2 \text{tr} \int \frac{d^4 k}{(2\pi)^4} (\not{p} + \not{k} + m)(\not{k} + m)(-2\pi) \\
&\quad \times \left[ \frac{i}{(p+k)^2 - m^2} \delta(k^2 - m^2) \sin^2 \theta_{k_0} \right]
\end{aligned}$$

$$\begin{aligned}
& + \frac{i}{k^2 - m^2} \delta((p+k)^2 - m^2) \sin^2 \theta_{p_0+k_0}] \\
= & 8i \left(\frac{m}{f_d}\right)^2 \int \frac{d^4 k}{(2\pi)^3} \left[ \frac{p \cdot k + 2m^2}{p^2 + 2p \cdot k} + \frac{-p \cdot k + 2m^2}{p^2 - 2p \cdot k} \right] \delta(k^2 - m^2) \sin^2 \theta_{k_0} \\
= & 8i \left(\frac{m}{f_d}\right)^2 \int \frac{dk_0 dx}{(2\pi)^3} \bar{k} d\bar{k}^2 \left[ \frac{Ek_0 - \bar{p}\bar{k}x + 2m^2}{p^2 + 2Ek_0 - 2\bar{p}\bar{k}x} \right. \\
& \left. + \frac{-Ek_0 + \bar{p}\bar{k}x + 2m^2}{p^2 - 2Ek_0 + 2\bar{p}\bar{k}x} \right] \delta(k^2 - m^2) \sin^2 \theta_{k_0} \\
= & -i \left(\frac{m}{f_d}\right)^2 \frac{1}{\pi^2} \int dk_0 \bar{k} \left[ 2 + \frac{p^2 - 4m^2}{4\bar{p}\bar{k}} \ln\left(\frac{p^2 + 2Ek_0 - 2\bar{p}\bar{k}}{p^2 + 2Ek_0 + 2\bar{p}\bar{k}}\right) \right. \\
& \left. - \frac{p^2 - 4m^2}{4\bar{p}\bar{k}} \ln\left(\frac{p^2 - 2Ek_0 + 2\bar{p}\bar{k}}{p^2 - 2Ek_0 - 2\bar{p}\bar{k}}\right) \right] \quad (52)
\end{aligned}$$

In the large dilaton mass limit,

$$\begin{aligned}
- i\Sigma_\chi^{(5)}(p^2) & \cong -i \frac{8}{\pi^2} \left(\frac{m}{f_d}\right)^2 \int dk_0 \bar{k} \left[ \frac{m^2}{p^2} - \frac{1}{3p^4} (\bar{p}^2 \bar{k}^2 + 3E^2 k_0^2) \right] \times \sin^2 \theta_{k_0} \\
& \cong -i \frac{8}{\pi^2} \left(\frac{m}{f_d}\right)^2 \int dk_0 \bar{k} \left[ \frac{m^2}{p^2} - \frac{E^2 k_0^2}{p^4} \right] \\
= & -i \frac{m^2}{m_\chi^2} \frac{8}{\pi^2} \left(\frac{m}{f_d}\right)^2 \left[ \frac{1}{2} \theta(\mu - m) (\mu \sqrt{\mu^2 - m^2} - m^2 \ln\left(\frac{\mu + \sqrt{\mu^2 - m^2}}{m}\right)) \right. \\
& - \frac{E^2}{m_\chi^2} \left( \frac{\mu(\mu^2 - m^2)^{3/2}}{4m^2} + \frac{\mu \sqrt{\mu^2 - m^2}}{8} \right) \\
& \left. - \frac{m^2}{8} \ln\left(\frac{\mu + \sqrt{\mu^2 - m^2}}{m}\right) \right] \quad (53)
\end{aligned}$$

where  $\bar{p}$  and  $\bar{k}$  denote  $|\vec{p}|$  and  $|\vec{k}|$  respectively, and  $p^2 = m_\chi^2$  is used.

## Figure Captions

Fig.1 Self-energy diagrams for pions. Solid lines represent the constituent quarks and dashed lines are for pions.  $D(F)$  represents thermal(Feynman) propagator.

Fig.2 Tadpole type diagram for quark. Solid lines represent the constituent quarks and wavy lines are  $\chi$ -field respectively.

Fig.3 Self-energy diagram for quark. Solid lines represent the constituent quarks. Dashed and wavy lines are for pions and  $\chi$ -field respectively.

Fig.4 Tadpole type diagram for  $\chi$ -field. Solid lines and wavy lines represent the constituent quarks and  $\chi$ -field respectively.

Fig.5 Self-energy diagram for  $\chi$ -field. Solid lines represent the constituent quarks and wavy lines are for  $\chi$ -field.

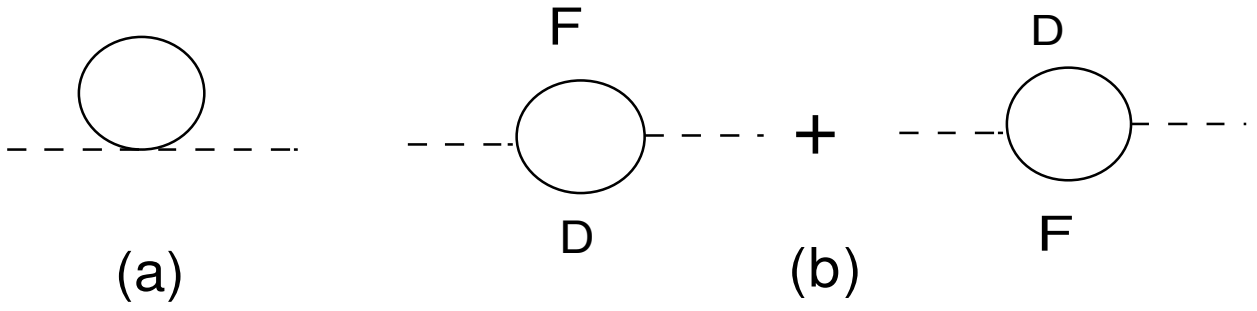


Fig.1

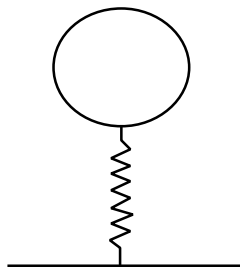


Fig.2

